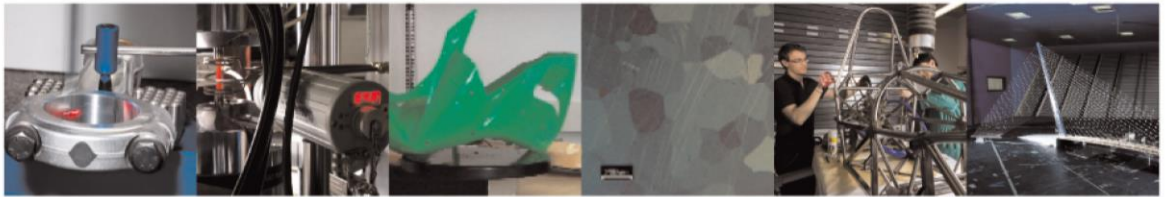




POLITECNICO
MILANO 1863

DIPARTIMENTO DI MECCANICA



On the Effectiveness of Profile Monitoring to Enhance Functional Performance of Particleboards

Colosimo, B. M., Meneses, M., and Semeraro, Q.

This is the peer reviewed version of the following article: Colosimo, B. M., Meneses, M., and Semeraro, Q. (2015) On the Effectiveness of Profile Monitoring to Enhance Functional Performance of Particleboards. *Qual. Reliab. Engng. Int.*, 31: 1665–1674, which has been published in final form at <https://doi.org/10.1002/qre.1699>. This article may be used for non-commercial purposes in accordance with Wiley Terms and Conditions for Use of Self-Archived Versions.

This content is provided under [CC BY-NC-ND 4.0](https://creativecommons.org/licenses/by-nc-nd/4.0/) license



On the effectiveness of profile monitoring to enhance functional performance of particleboards

Bianca M. Colosimo^{a*}, Marcela Meneses^b and Quirico Semeraro^a.

^aDipartimento di Meccanica, Politecnico di Milano, via La Masa 1- 20156 Milano, Italy

^bEscuela de Ingeniería en Producción Industrial, Instituto Tecnológico de Costa Rica, Cartago, Costa Rica

*Corresponding author, E-mail address: biancamaria.colosimo@polimi.it

Abstract

This paper explores connection between profile monitoring and functional performance of manufactured products. In particular, the empirical relationship between the vertical density profile of the particleboards and their functional performances (the internal bond and the surface soundness) is studied. Results based on a real case study showed that the profile shape clearly affects the final performance of the panel and thus profile monitoring is really worth to keep the final quality of the product at its target level.

This result motivates the second objective of the paper, which consists of comparing performance of two (parametric and nonparametric) approaches for vertical density profile monitoring.

1 Introduction

Profile monitoring consists of monitoring the functional relationship between a response variable and one or more explanatory variables, with the idea of controlling the product or process quality. Applications of functional data include calibration studies, geometric specification monitoring and process signal control (see Woodall¹ and the recent book by Noorossana et al.²).

Despite of the large attention paid to profile monitoring in recent literature, most of the proposed approaches focused on presenting new methods and tools to perform statistical profile monitoring. Up to authors' knowledge, not many studies focused on studying connection between the monitored profile and the final product quality. The first aim of the present paper is to investigate the relationship between the profile shape and the product performance, with respect to a typical test case in the literature on profile monitoring, namely the vertical density profiles (VDPs) of particleboards produced in the wood composites industry. To this aim, we will first model the VDP using a parametric model and then we will link the model coefficients to the functional performance of the produced product. Among models to represent VDP as functional data, Winistorfer et al.³ considered spline regression, Xu and Winistorfer⁴ presented a model based on Fourier basis while Walker and Wright⁵ used additive models. In our study, the VDP profile will be modeled by combining B-spline regression (to represent the large scale pattern) and autoregressive model (to represent the autocorrelated error terms) – B-spline+AR. As a matter of fact, after removing the main pattern modeled via B-spline, all the real data showed a remaining autocorrelation structure and this is why a model combining B-spline with autocorrelation was assumed. A similar need was observed in many different applications of profile monitoring⁶⁻⁹.

In order to check whether profile changes affect the particleboard final quality, we will take as reference a real case study, where a set of particleboards are produced and their VDPs inspected while producing. Starting from the literature¹⁰⁻¹¹ on particleboards production, we will consider the internal bond and the surface soundness as quality characteristics of interest.

After exploring the strong connection between profile shape and product performance, we will then compare performance of two different methods for VDP monitoring.

In the literature on VDP profile monitoring, different approaches have been proposed to develop a monitoring policy. In particular, Williams et al.¹² considered profile monitoring via nonlinear regression, Chang and Yadama¹³ used splines, supported by wavelets filtering, in order to develop a profile monitoring method. Fan et al.¹⁴ proposed breaking the complete profile into several segments in order to monitoring them separately. Wei et al.¹⁵ proposed a nonparametric model to detect local shifts, local shape distortion and overall shape deviation of the VDP pattern. Horng et al.¹⁶ provided a monitoring schemes based on nonparametric regression.

In our paper, two different monitoring approaches will be considered and compared. The first approach will take advantage of the B-spline+AR model developed to represent the profile pattern and combine it with a multivariate control chart for monitoring the model coefficients and a univariate control chart to monitor the residual variance. A second nonparametric approach proposed by Qiu et al.¹⁷ will be used as competitor method. Performances of the different methods will be evaluated in terms of Average Run Lengths (ARLs) observed on different realistic out-of-control states. Final remarks will be drawn.

The remainder of the paper is organized as follows. In Section 2 we will present the real case study. Section 3 will explore relationship between the VDP shape and the final performance of the particleboard. Section 4 and 5 will describe the competitive approaches for profile monitoring while Section 6 will present the performance comparison. Section 7 will eventually present the conclusions.

2 The Real Case Study: particleboards

Wood composites is a general term for a variety of different board products, which have an impressive range of engineering properties. The term particleboard is used to define any panel product that is made with wood particles¹⁰. In order to achieve the desired properties of the final product, the manufacturing process can be adjusted accordingly. Requirements such as density, strength and durability are defined in the international standards¹⁸⁻²² together with the related measuring methods. Particleboard manufacturing is a complex process which consists of bonding together the wood particles by adding synthetic adhesives and then pressing them at high pressures and temperatures^{23, 24}. This literature points out that the critical operation in the particleboard manufacture are the mattress formation and the hot pressing. The amount and state of material in the mattress formation determine the average board density, whereas the pressing technique is the main element defining the functional behavior of the density along the thickness. During hot-pressing process, the interaction among heat, moisture and pressure gives rise to non-uniform deformation of the elements, which results in an uneven density distribution along the thickness²⁵. Figure 1 plots the VDP, with the density being considered as a response variable and the correspondent measured location acting as explanatory variable.

[Insert Figure 1 about here].

The VDP curve is influenced by the process conditions and changes of its shape could affect the mechanical characteristics of the final product. The international standards define some specific

mechanical requirements, namely the internal bond (IB), the surface soundness (SS) and the bending strength (BS), together with the way in which measurements should be performed. IB is the resistance to a stress acting perpendicularly to the panel plane and it is determined by the maximum load related to the surface area of the specimen²⁰. SS is the bonding strength between the particles at the panel surface and the material below. For its measurement, a shallow circular groove is cut on the specimen surface and a steel pad is bonded to the area within the groove. The tensile load required to pull this pad from the surface is measured²¹. The bending strength is computed as the ratio of the bending moment at the maximum load²⁷

Different authors have focused their attention on the relationship between the process and the mechanical properties of the final product^{23, 24, 28}. We want to consider this relationship from a different viewpoint, linking the panel properties to the VDP shape instead that connecting them to the process parameters.

2.1 Data set description

The j^{th} VDP is summarized in a vector $\mathbf{y}_j = (y_{1j}, \dots, y_{tj}, \dots, y_{nj})^T$ of densities ($j = 1, 2, \dots, J$), measured at a set of n equally spaced locations $\mathbf{x} = (x_1, \dots, x_t, \dots, x_n)^T$. Figure 1 represents a generic VDP, where y_{tj} is the density (kg/m^3) measured at thickness (mm) t on the j^{th} panel profile. In our real case study, the VDP sample was measured by using a profilometer that takes measurements at fixed depths across the thickness of the board. The reference sample is a set of $J = 263$ profiles made of $n = 189$ observations, where each measurement is taken at a fixed distance of $0.09 mm$.

3 Relationship between VDP shape and particleboard mechanical properties

In order to explore the relationship between the mechanical properties of the panel and the VDP, we will start focusing on a parametric model for the VDP. Then we will explore possible connection between the model coefficients and the mechanical properties, namely the IB and the SS. This relationship will be estimated via regression analysis.

3.1 Modeling VDP

We will assume that the j^{th} VDP can be represented as:

$$\mathbf{y}_j = \mathbf{s}_j(\mathbf{x}) + \mathbf{v}_j \quad (1)$$

where $\mathbf{s}_j(\mathbf{x})$ is a large-scale model based on cubic B-spline regression while $\mathbf{v}_j = (v_{1j}, \dots, v_{tj}, \dots, v_{nj})'$ represents the small-scale component, modeled as autocorrelated errors. We will assume a *ARMA* (p, q), autoregressive moving average model for residuals observed at location t on the j^{th} profile:

$$v_{tj} = a_{1j}v_{t-1,j} + \dots + a_{pj}v_{t-p,j} + \varepsilon_{tj} - m\varepsilon_{t-1,j} - \dots - m_{qj}\varepsilon_{t-q,j} = \frac{M_{qj}(B)}{A_{pj}(B)} \varepsilon_{tj}$$

where $M_{qj}(B) = 1 - m_{1j}B - \dots - m_{qj}B^q$, $A_{pj}(B) = 1 - a_{1j}B - \dots - a_{pj}B^p$ and $B^k x_t = x_{t-k}$.^{29, 30} is the backshift operator. Final residual errors ε_{tj} 's are assumed to be independent, with zero mean and constant variance, $\varepsilon_j \sim (\mathbf{0}, \sigma^2 \mathbf{I})$.

In order to define the large-scale model, the interval $[X_{min}, X_{max}]$ is partitioned in L subintervals, separated by $L - 1$ internal knots $X_{min} = \tau_0 < \tau_{1j} \leq \tau_{2j} \leq \dots \leq \tau_{L-1j} < \tau_{Lj} = X_{max}$. The knot vector $\boldsymbol{\tau}_j$ uses the subindex j because at least in principle, different knot locations can be identified for each profile. The function $\mathbf{s}_j(\mathbf{x})$ is a linear combination of cubic B-spline basis functions

$$\mathbf{s}_j(\mathbf{x}) = \sum_{k=1}^r \mathbf{B}_k(\boldsymbol{\tau}_j; \mathbf{x}) \mathbf{c}_j.$$

where $\mathbf{B}_k(\boldsymbol{\tau}_j; \mathbf{x})$ is the $(n \times r)$ B-spline matrix with internal knot vector $\boldsymbol{\tau}_j = \{\tau_{1j}, \tau_{2j}, \dots, \tau_{L-1j}\}$ which depends on the profile index j and $\mathbf{c}_j = (c_{1j}, c_{2j}, \dots, c_{rj})'$ are the $r = 4 + L - 1$ coefficients to be estimated.

In order to select the number and the position of the knots together with the autocorrelation structure of the noise terms, a set of competitor models was identified and ranked according to the Akaike's Information Criterion (AIC)²⁹.

In particular, two solutions were considered for knots placing. The first one assumes a uniform knot placement (i.e., the subinterval between knots is fixed and constant for all the profiles). A set of 20 internal knots were considered for all the profiles. The second strategy consists of optimizing the knots position for the mean profile., using the `curfit.free.knots` procedures of the `DierckxSpline` library implemented in the R software^{31, 32}. In this case, the maximum number of internal knots to be placed was fixed to 11, provided that any increase of the knot number did not seem to improve the model AIC. Eventually, $AR(p)$ models with p ranging from 2 to 4 were considered as possible solutions. The System identification toolbox in Matlab³⁰ was used to estimate all the large- and small-scale coefficients at the same time and to compute the AIC indicator for all the competitive models (considering both the uniform and the optimized knot placing strategies and the different orders of the $AR(p)$ model). Clearly, only models corresponding to uncorrelated final noise terms were considered as viable solutions. Eventually, the final model corresponds to the combination ($r = 8$, $p = 4$) with uniform knot placement (i.e., the subinterval between knots ($\boldsymbol{\tau}$) is fixed and constant for all the profiles) and an $AR(4)$ for the small-scale component

$$\mathbf{y}_j = \sum_{k=1}^8 \mathbf{B}_k(\boldsymbol{\tau}; \mathbf{x}) \mathbf{c}_j + \mathbf{v}_j$$

$$v_{tj} = \frac{1}{1 - a_{1j}B - a_{2j}B^2 - a_{3j}B^3 - a_{4j}B^4} \varepsilon_{tj} \quad j = 1, \dots, J; t = 1, \dots, n \quad (2)$$

characterized by a set of $d = r + p = (8) + 4 = 12$ parameters to be estimated.

3.2 Effect of the VDP shape on the panel properties

In order to understand the relationship between the VDP shape and the panel properties, we linked the panel properties to the VDP model coefficients shown in Eq. 2, (namely $\hat{c}_{1j}, \dots, \hat{c}_{8j}, \hat{a}_{1j}, \dots, \hat{a}_{4j}, \sigma_j^2$ for the j -th profile), acting as regressors. Results of this analysis are shown and discussed in the following.

3.2.1 Internal Bond analysis

For each of the 100 panels, we measured the density along the thickness and used the model in Eq.2 to estimate the unknown coefficients. The Internal Bond (IB) was then measured on the same panel, using existing standards^{20, 21}.

Results of the regression analysis are shown in Table 1, where the variance inflation factors (VIF) is shown together with the ANalysis Of the Variance (ANOVA) table, which shows that some of the VDP coefficients affects the IB property. As clear from Table 1, the IB is significantly affected by the large-scale VDP pattern via coefficients $\hat{c}_{4j}, \hat{c}_{5j}$ and \hat{c}_{6j} . Also the small-scale model of the VDP affects the IB property, considering the first autoregressive term \hat{a}_{1j} is significant. The VIFs show that there is no multicollinearity among the regressors. Assumptions on residual errors (normality and lack of autocorrelation) are also verified.

Figure 2 shows the in-control pattern together with a second profile, where parameters $\hat{c}_{4j}, \hat{c}_{5j}, \hat{c}_{6j}$ are perturbed (considering a shift size of 1.5, -1 and -1 standard deviation unit, respectively). The parameter \hat{a}_{1j} is reduced at 0.8 but this coefficient does not influence the profile shape. As a matter of fact, Figure 2 shows how the central part of the profile is mainly responsible of the IB property.

[insert Table 1 about here]

[insert Figure 2 about here]

The significance of the autoregressive term suggests the influence of the particle size on the tensile strength, which probably increases as the homogeneity of the wood particles increases²⁸.

3.2.2 Surface soundness analysis.

Similarly to the IB analysis, surface soundness (SS) was linked to the VDP constructing an empirical model built on the sample of 100 profiles. Results are shown in Table 2. In this case, significant parameters are $\hat{c}_{4j}, \hat{c}_{5j}, \hat{c}_{6j}$ and \hat{c}_{7j} . Also in this case, assumptions on residuals were verified. Figure 3 represents the results of this analysis, showing the effect of changes of significant coefficients (considering a shift of 1.5, -1, -1 and -1 standard deviation for $\hat{c}_{4j}, \hat{c}_{5j}, \hat{c}_{6j}$ and \hat{c}_{7j} , respectively).

[insert Table 2 about here]

[insert Figure 3 about here]

Also in this case, the central part of the profile affects the SS property. However, an addition effect is visible, connecting the SS to the border area between the surface layer and the inner layer. This result is consistent with results presented in the literature²⁴, where it is shown that a larger density in the zone subject to the higher stress can result in improved mechanical properties of the panel.

As a concluding remark, the performed analysis showed that the VDP pattern affects the functional properties of the panel. This results is particularly important, since it gives relevance to profile monitoring. In order to avoid deteriorated product performance, the shape of the density profile should be monitored with time.

4 Monitoring scheme

For monitoring purpose, the coefficients $\mathbf{Z}_j = (z_{1j}, \dots, z_{dj})^T = (c_{1j}, \dots, c_{8j}, a_{1j}, \dots, a_{4j})^T$ of the profile model in Eq.2, can be monitored via a Hotelling T^2 control chart:

$$T_j^2 = (\mathbf{Z}_j - \hat{\boldsymbol{\mu}}_z)' \hat{\boldsymbol{\Sigma}}_z^{-1} (\mathbf{Z}_j - \hat{\boldsymbol{\mu}}_z) \quad (3)$$

where $\hat{\boldsymbol{\mu}}_z = [\bar{z}_1, \dots, \bar{z}_d]^T$ is the vector of sample means, whilst $\hat{\boldsymbol{\Sigma}}_z^{-1}$ is the inverse of the (short-run) estimate of the covariance matrix, given by

$$\hat{\boldsymbol{\Sigma}}_z = \frac{1}{2} \frac{\mathbf{V}'\mathbf{V}}{J-1} \quad (4)$$

where \mathbf{V} is the $(J-1) \times d$ matrix consists of row vectors of the differences $v_j = z_{j+1} - z_j$ with $j = 1, 2, \dots, J-1$.

A second control chart is designed to monitor the variance σ_j^2 of the residual terms $\boldsymbol{\varepsilon}_j$'s.

In order to design the two control charts (the T^2 + Shewhart control charts for the residual variance), a first type error of $(1 - \sqrt{1 - \alpha'})$ was set for each of the two charts. This was made in order to achieve an overall nominal false alarm rate equal to $\alpha' = 0.05$.

To design the control limits, a bootstrapping procedure was used considering that the non-normal distribution of residual terms does not allow one to use the analytical results of the T^2 and Shewhart control charts for the error variance. Starting from the first set of $J = 263$ real profiles, we assumed the average VDP computed on 7 profiles as the reference VDP to be monitored and we performed bootstrapping to generate 20000 replications of VDPs. Then, we compute the empirical distribution of the monitored statistics and the related control limits for the procedure.

4.1 Performance Evaluation

Performance of the monitoring procedure was computed considering the average number of samples to detect out-of-control states of the VDP production process (i.e., the Average Run Length - ARL). In order to define possible out-of-control conditions, we linked the profile changes to one or more special causes, which can cause these conditions to happen, according to literature on VDP production. We will consider five out-of-control scenarios described in Table 3. These cases were generated by opportunely perturbing the parameters of Eq.2, in order to introduce changes in the

general pattern (scenario A, B and C of Table 3) or in the autocorrelation structure of the profiles (scenarios D and E of Table 3). Figure 4 presents the first three scenarios.

[insert Table 3 about here]

[insert Figure 4 about here]

4.1.1 Results

For each scenario listed in Table 3, performance of the monitoring procedure was computed using as indicator the average run length (ARL) required to detect the specific out-of-control condition assumed in that scenario. A set of 10000 run lengths were collected for each scenario before computing the average, shown in Table 4.

[insert Table 4 about here]

The results of Table 4 denote that the approach is effective in detecting out-of-control states. For all the scenarios, the monitoring procedure detects the out-of-control condition at the first sample on average, except for scenario B, where almost two samples are required instead.

5 Alternative monitoring procedure

5.1 The nonparametric mixed effect model (NPME) for profile monitoring.

Following Qiu et al.¹⁷ we assumed the following nonparametric mixed-effects model for the VDP

$$y_{tj} = g(x_t) + f_j(x_t) + \varepsilon_{tj}, \quad j = 1, \dots, J, \quad t = 1, \dots, n \quad (5)$$

where y_{tj} is the observed response (density) of profile j at the location point x_t along the thickness; $g(x_t)$ models the population mean function (the fixed effect) and $f_j(x_t)$ represents the individual curve deviation from $g(x_t)$ (the random-effects) curve. ε_{tj} 's are measurement errors with zero mean variance σ_j^2 .

Following the approach by Qiu et al.¹⁷, Fan and Gijbels³³ and Wu and Zhang³⁴, $g(\cdot)$ and $f_j(\cdot)$ can be estimated by combining linear mixed effects models and local polynomial techniques, considering an iterative procedure. Let $\hat{\mathbf{f}}_j(\mathbf{x}) = (\hat{f}_j(x_1), \dots, \hat{f}_j(x_n))^T$ represent the random effects predicted for profile j at a set of locations $\mathbf{x} = (x_1, \dots, x_n)^T$, which are assumed to be constant for all the profiles. A multivariate Hotelling's T^2 control chart can be eventually built on these predicted values of the random effect :

$$T_j^2 = \hat{\mathbf{f}}_j^T(\mathbf{x}) \widehat{\Sigma}_f^{-1} \hat{\mathbf{f}}_j(\mathbf{x}) \quad (6)$$

where $\widehat{\Sigma}_f^{-1}$ is the inverse of the variance-covariance matrix computed as $\widehat{\Sigma}_f = 1/2(J-1) \sum_{j=1}^{J-1} (\hat{f}_{j+1} - \hat{f}_j) (\hat{f}_{j+1} - \hat{f}_j)^T$.

Residuals computed as

$$\hat{\varepsilon}_{tj} = y_{tj} - \hat{g}(x_t) - \hat{f}_j(x_t)$$

Are used to estimate the residual variance $\hat{\sigma}_j^2$, which is monitored using a traditional Shewhart's control chart. In order to design the two control charts, a first type error of $\alpha = (1 - \sqrt{1 - \alpha'})$ is set for each chart ($\alpha' = 0.05$). Eventually, the empirical distributions of the monitored statistics, T_j^2 and $\hat{\sigma}_j^2$ were computed to define the control limits.

5.2 Results

Starting from the real case study, control limits of both the parametric and nonparametric approaches were computed starting from the empirical distributions of the statistics to be monitored. In particular, the average of 7 real profiles was used as reference VDP to be monitored. Bootstrapping was used to generate 20000 replications of the reference profiles and the empirical distributions of the statistics of interest were computed to design the control limits.

The performance of the competing procedures were then computed using the average run length (ARL_1) as indicator. Table 5 shows the average and the standard deviation (in parenthesis) of 10000 run lengths collected for each scenario.

[insert Table 5 about here]

The results of Table 5 denote that the nonparametric approach is effective in detecting out-of-control states. Performances are similar to the ones obtained by the B-spline+AR parametric approach and this is why a further comparison between the two methods was eventually carried out.

6 Simulation and comparative studies

In order to compare the performance of both the VDP monitoring procedures, we simulated different sizes for all the shifts in order to compute the operating characteristic (OC) curve, i.e., a plot of the probability β of not detecting the change as a function of the change size. Recall that β is related to ARL_1 , as $ARL_1 = \frac{1}{1 - \beta}$.

For all the out-of-control scenarios of Table 3, the whole shift shown in Table 3 was divided in 7 or 8 or 7 equally sized step changes. For example, in scenario A, where the whole shift is given by increasing coefficients (c_2, c_3, c_8, c_9) by $(-1, -2, -2, -1)$, the first step change consists of adding to the in-control coefficients $1/8$ of the whole shift size, i.e., $(-0.125, -0.250, -0.250, -0.125)$. In the following, l will be used as indicator of the shift size, ranging from $l = 0$ (meaning no changes) to $l = 1$ (meaning the whole change shown in Table 3). Figures 5 to 9 show the OC curves computed using the parametric or the nonparametric approach in all the out-of-control scenarios.

[insert Figure 5 about here]

[insert Figure 6 about here]

[insert Figure 7 about here]

[insert Figure 8 about here]

[insert Figure 9 about here]

Figures 5-9 show that both the monitoring approaches are effective in detecting out-of-control states. The nonparametric approach seems to perform better or equally better than the parametric method in most of the cases. The only exception is scenario B and A when for small shifts the parametric method outperforms the nonparametric one.

7 Conclusions

We investigated the relationship between the VDP shape and the strength properties (IB and SS) of the particleboard panel. Our study showed that these relationships exist. In particular, the IB depends significantly on the density of the central zone or core density of the panel. Also for the SS, the central part of the profile is critical, but an addition effect of the borders is visible.

With respect to a real case study, we further explored performances of two promising approaches for complex profile monitoring with autocorrelated errors. We concluded that the type of profile shape does not seem to influence the performance of the monitoring procedure in use. Analyzing the results obtained from the comparison, we resolve that it is difficult to choose a particular method for monitoring VDP because both the parametric and the nonparametric approaches present several advantages. They detect out-of-control states and have a satisfactory performance. They perform well for changes in both the mean and the correlation structure of VDP. The preference for one approach or the other depends on the type of shift (shift in the curve or shift in correlation structure) or the shift size.

References

1. Woodall WH. Current research on profile monitoring. *Produção*, 2007, 17, pp.420-425.
2. Noorossana R.R., Saghei A., and Amiri A., eds. 2012. *Statistical Analysis of Profile Monitoring*, Wiley.
3. Winistorfer PM, Young TM, Walker E. Modelling and Comparing Vertical Density Profiles. *Wood and Fiber Science* 1996; **28**(1):133-141.
4. Xu W, Winistorfer PM. Fitting an equation to vertical density profile using Fourier analysis. *Holz als Roh-und Werkstoff* 1996; **54**: 57-59.
5. Walker E, Wright S. Comparing Curves Using Additive Models. *Journal of Quality Technology* 2002; **34**:118-129.

6. B.M. Colosimo, M. Pacella and Q. Semeraro, 2008, Statistical Process Control for Geometric Specifications: On the Monitoring of Roundness Profiles, *Journal of Quality Technology*, vol. 40, number 1, January 2008, pp. 1-18.
7. B.M. Colosimo and M. Pacella, 2010, A Comparison Study of Control Charts for Statistical Monitoring of Functional Data, *International Journal of Production Research*, Vol. 48, number 6, 1575–1601.□
8. Jensen, W. A., Birch, J. B., & Woodall, W. H. (2008). Monitoring correlation within linear profiles using mixed models. *Journal of Quality Technology*, 40(2), 167-183.
9. Noorossana, R., Amiri, A., & Soleimani, P. (2008). On the monitoring of autocorrelated linear profiles. *Communications in Statistics—Theory and Methods*, 37(3), 425-442.
10. Thoemen H, Irle M, Sernek M. *Wood-Based Panels - An Introduction for Specialists*. Brunel University Press: London, 2010.
11. Kelly MW. Critical review of relationships between processing parameters and physical properties of particleboard. Department of Agriculture, Forest Service, Forest Products Laboratory: Madison, <http://www.fpl.fs.fed.us/documnts/fplgtr/fplgtr10.pdf>.
12. Williams JD, Woodall WH, Birch JB. Statistical monitoring of nonlinear product and process quality profiles. *Quality and Reliability Engineering International* 2007; **23**(8): 925–941.
13. Chang SI, Yadama S. Statistical process control for monitoring non-linear profiles using wavelets filtering and B-spline approximation. *International Journal of Production Research* 2010; **48**(4):1049-1068.
14. Fan S-K S, Yao N-Ch, Chang Y-J, Jen Ch-H. Statistical monitoring of nonlinear profiles by using piecewise linear approximation. *Journal of Process Control* 2011; 21:1217-1229.
15. Wei Y, Zhao Z, Lin D. Profile control chart based on nonparametric L-1 regression methods. *The Annals of Applied Statistics* 2012; **6**(1):409–427.
16. Horng J-J, Huang H-L, Lin S-H, Tsai M-Y. Monitoring nonlinear profiles with random effects by nonparametric regression. *Communications in Statistics* 2009; **38**:1664-1679.
17. Qiu P, Zou Ch, Wang Z. Nonparametric profile monitoring by mixed effects modeling. *Technometrics* 2010; **52**:265-277.
18. ISO 16893-1:2008. *Wood-based panels — Particleboard — Part 1: Classifications*.
19. ISO 16893-2:2010. *Wood-based panels — Particleboard — Part 2: Requirements*.
20. ISO 16984:2003. *Wood-based panels — Determination of tensile strength perpendicular to the plane of the panel*.
21. ISO 16981:2003. *Wood-based panels — Determination of surface soundness*.
22. ISO17064:2004. *Wood-based panels - Fibreboard, particleboard and oriented strand board (OSB) – Vocabulary*.

23. Thoemen H., Irle M., and Sernek M., Wood-Based Panels - An Introduction for Specialists. London: Brunel University Press, 2010.
24. Kelly M.W., "Critical review of relationships between processing parameters and physical properties of particleboard," Madison, WI: U.S. Department of Agriculture, Forest Service, Forest Products Laboratory.
25. Wong ED. Effects of density profile on the mechanical properties of particleboard and fiberboard. Wood Res 1999; **86**:19-33.
26. Wong E-D, Zhang M, Wang Q, Kawai S. Formation of the density profile and its effects on the properties of particleboard. Wood Science and Technology 1999; **33**:327-340.
27. Wong JY. Cooper PA. Effect of grain orientation and surface wetting on vertical density profiles of thermally compressed fir and spruce. Holz als Roh und Werkstoff 2005; **63**:397-402.
28. Geimer R, Montrey HM, Lehman WF. Effects of Layer Characteristics on the Properties Of Three-Layer Particleboards. Forest Products Journal 1975; **25**(3).
29. Box, G. E., Jenkins, G. M., & Reinsel, G. C. (2013). Time series analysis: forecasting and control. Wiley. com.
30. L. Lennart. System Identification Toolbox, User's Guide. The MathWorks, 1997.
31. de Boor C. Spline Toolbox. User's Guide, 2009.
32. Sundar DR. Spencer G. Package DierckxSpline, 2009.
33. Fan J, Gijbels I. Local Polynomial Modeling and Its Applications. Chapman & Hall: London, 1996.
34. Wu H, Zhang J-T. Local polynomial mixed effect models for longitudinal data. American Statistical Association: Theory and Methods 2002; **97**:883-897.

Tables

Table 1. Regression analysis linking the Internal Bond property to VDP model coefficients (100 profiles).

Predictor	Coef	SE Coef	T	P	VIF
Constant	-6,0039	0,6201	-9,68	0,000	
c4	0,32861	0,05664	5,80	0,000	1,120
c5	0,58403	0,06785	8,61	0,000	1,274
c6	0,11084	0,04586	2,42	0,017	1,353
a1	0,07747	0,02878	2,69	0,008	1,007

S = 0,0292186 R-Sq = 59,1% R-Sq(adj) = 57,4%

Analysis of Variance

Source	DF	SS	MS	F	P
Regression	4	0,124434	0,031108	36,44	0,000
Residual Error	101	0,086226	0,000854		
Total	105	0,210660			

Table 2. Regression analysis: SS as a function of the VDP coefficients.

Predictor	Coef	SE Coef	T	P	VIF
Constant	-9,3972	0,8184	-11,48	0,000	
c4	0,28101	0,07718	3,64	0,000	1,110
c5	0,66413	0,08775	7,57	0,000	1,391
c6	0,29297	0,06128	4,78	0,000	1,286
c7	0,40681	0,05541	7,34	0,000	1,409

S = 0,0349567 R-Sq = 70,7% R-Sq(adj) = 69,5%

Analysis of Variance

Source	DF	SS	MS	F	P
Regression	4	0,280764	0,070191	57,44	0,000
Residual Error	95	0,116087	0,001222		
Total	99	0,396851			

Table 3: Five out-of-control scenarios (BS: bending strength, IB: internal bond, SS: surface soundness).

	Coeff.	Values of the changes	Process change description, cause (C) and consequence (Cs)
A	c_2, c_3 c_8, c_9	-1, -2 -2, -1	Increased drop in the density between the surface layers and the middle layer. C: high temperature in the central area of the press or low speed pressing. Cs: reduce the value of SS.
B	c_4, c_5 c_6, c_7 c_8	1.5, -1 -1, -1 1.5	Increase of the density change between the surface layers and the middle layer. C: excessive moisture on the superficial layer, low press residence time or high speed pressure on entrance press. Cs: lack of cohesion of the middle layer of the particles (poor IB).
C	$c_1, c_2,$ c_3, c_4 c_5, c_6 c_7, c_8 c_9, c_{10}	-1.5, -1, -1, 1, 1.4, 1.4, 1, -1, -1, -1.5	Density gradient reduced (reduction of outer layers density and increase in inner layer density). C: excessive time spent in the press or poor surface moisture of the faces. Cs: facilitate the improvement of the IB but causes a deterioration in BS.
D	σ^2	x 1.25 ²	Increasing variance of the noise term. C: change in particle wood size. Cs: higher 'roughness' of the profile that can affect the board strength.
E	a_{1j}, a_{2j} a_{3j}, a_{4j}	x 0.8	Reduced intensity of the autocorrelation coefficients (alteration of particles wood size). Apply the remarks made in D.

Table 4 ARL results in all the simulated scenarios listed in Table. 3.

Monitoring procedure	<i>ARL₁ in all the simulated scenarios</i>				
	<i>A</i>	<i>B</i>	<i>C</i>	<i>D</i>	<i>E</i>
S+ARMA with fixed knot profile monitoring	1.1634 (0.0044)	2.0192 (0.0141)	1.0837 (0.0030)	1.0098 (0.0010)	1.1715 (0.0041)

Table 5: ARL₁ results in all the simulated scenarios listed in Table 3.

<i>scenario</i>	<i>A</i>	<i>B</i>	<i>C</i>	<i>D</i>	<i>E</i>
<i>ARL₁</i> (standard errors)	1.0118 (0.0011)	3.2244 (0.0265)	1.0000 (0.0000)	1.0140 (0.0012)	1.0021 (0.0005)

Figures

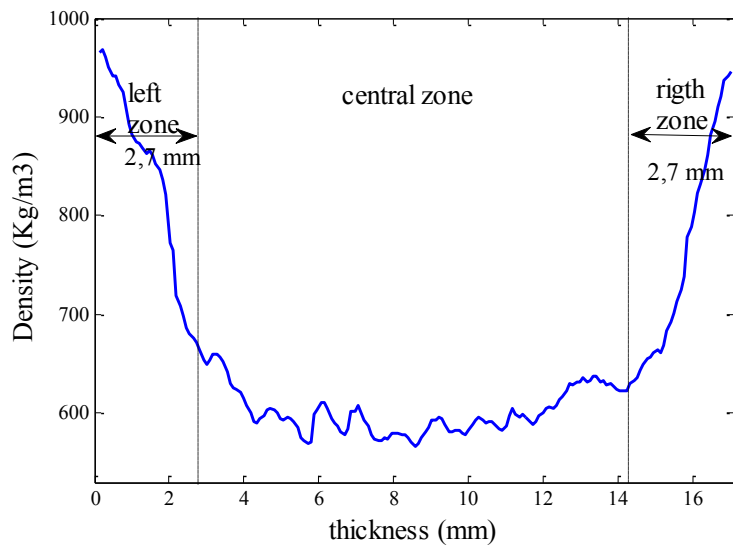


Figure 10: VDP (central, right and left zones).

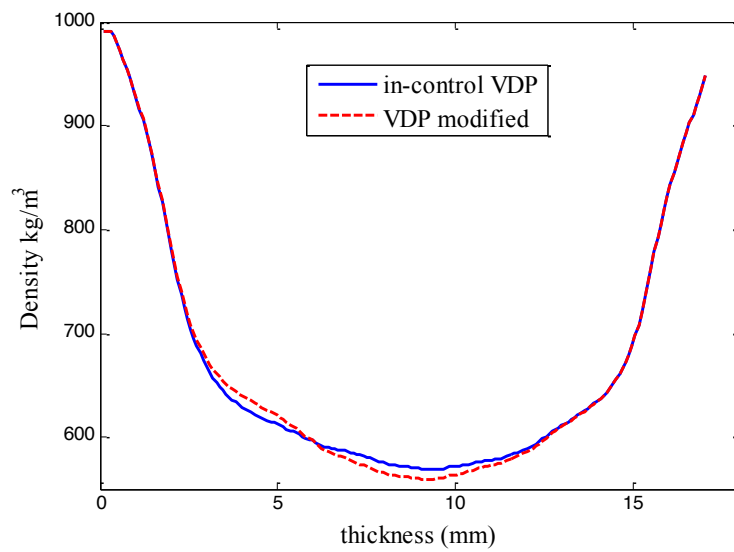


Figure 11: Effect of coefficients \hat{c}_{4j} , \hat{c}_{5j} , \hat{c}_{6j} and \hat{a}_{1j} on the VDP pattern.

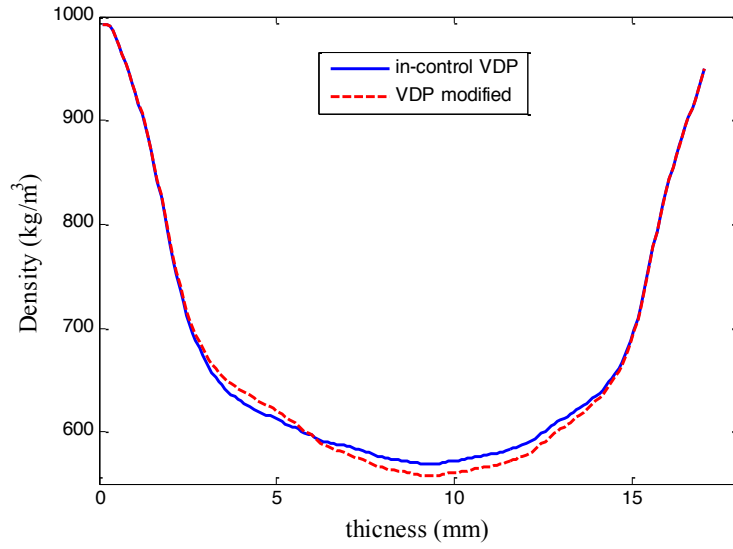
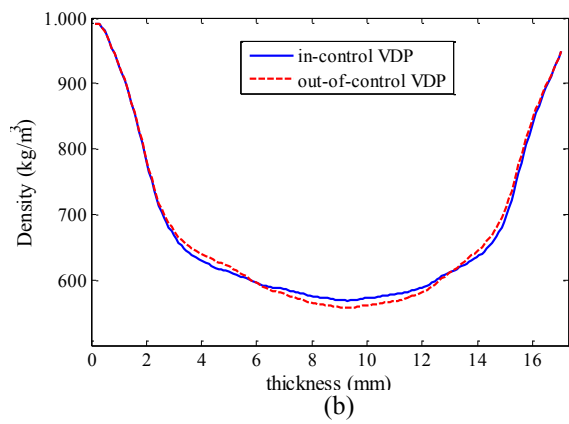
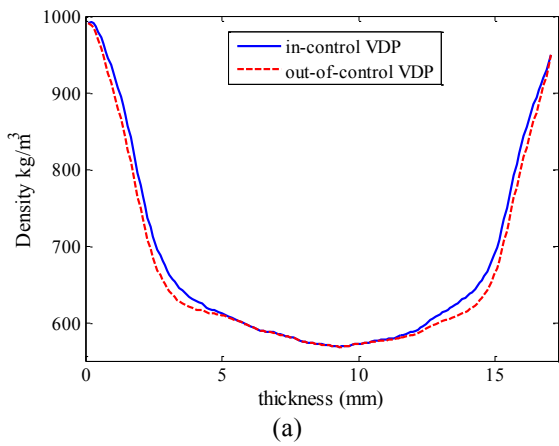
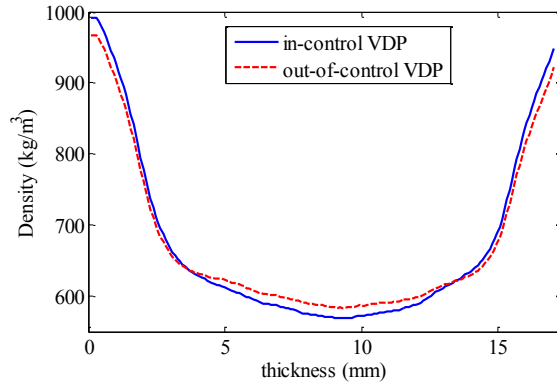


Figure 12: Effect of changes of coefficients \hat{c}_{4j} , \hat{c}_{5j} , \hat{c}_{6j} and \hat{c}_{7j} on the VDP pattern.





(c)

Figure 13. (a) out-of-control profile in accordance with scenario A, (b) out-of-control profile in accordance with scenario B, (c) out-of-control profile in accordance with scenario C.

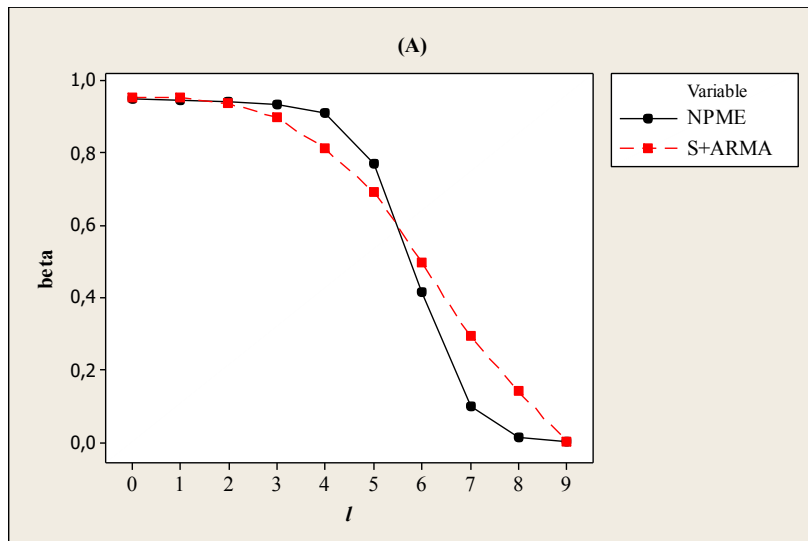


Figure 14: OC curve for the parametric (S+ARMA) and nonparametric (NPME) profile monitoring approaches for scenario A.

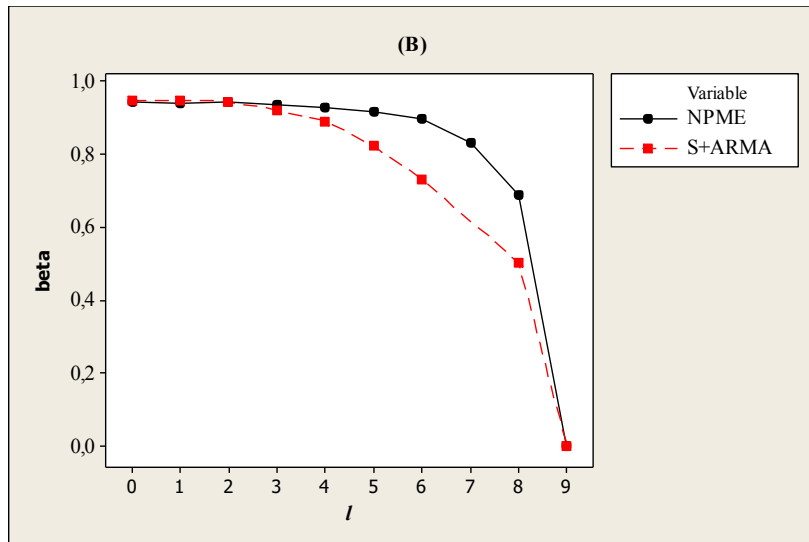


Figure 15: OC curve for the parametric (S+ARMA) and nonparametric (NPME) profile monitoring approaches for scenario B.

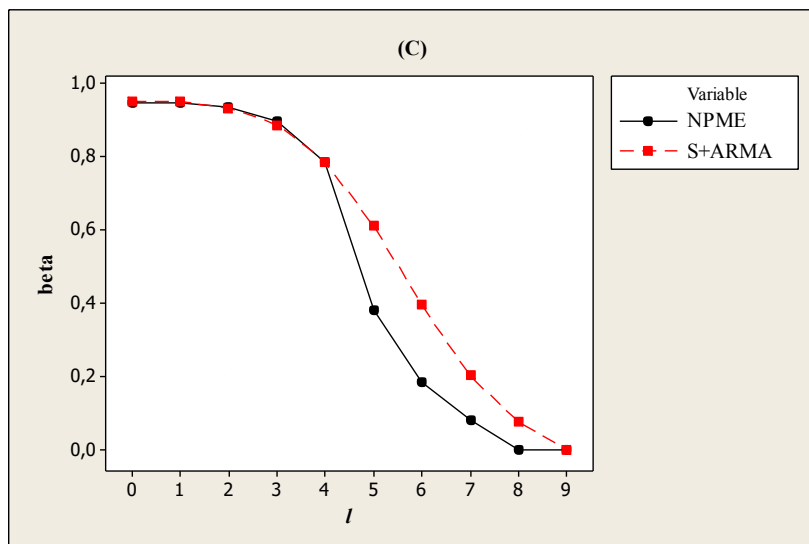


Figure 16: OC curve for the parametric (S+ARMA) and nonparametric (NPME) profile monitoring approaches for scenario C.

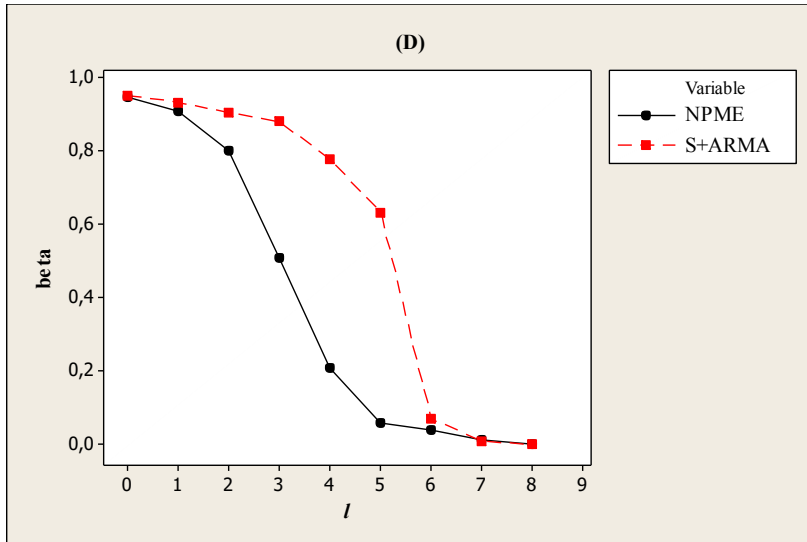


Figure 17: OC curve for the parametric (S+ARMA) and nonparametric (NPME) profile monitoring approaches for scenario D.

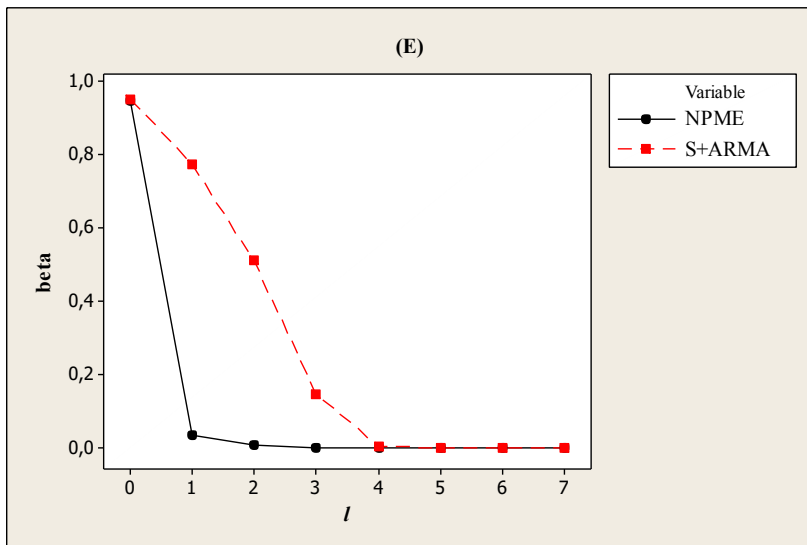


Figure 18: OC curve for the parametric (S+ARMA) and nonparametric (NPME) profile monitoring approaches for scenario E.